Size-Selective Effects on Fullerene Adsorption by Nanoporous Molecular Networks

Yong-Tao Shen, Ke Deng, Qing-Dao Zeng, and Chen Wang**

***A** new hierarchical self-assembling molecular template, which can size-selectively immobilize fullerene molecules, is reported. The molecular template is fabricated from 1,3,5-tris(10-carboxydecyloxy)benzene (TCDB) and triangle-shaped macrocycles. It is observed that the two-dimensional hydrogen-bonded achiral TCDB network affected by the 3NN-Macrocycle becomes a chiral network. Host and guest molecules both form chiral arrangements with hexagonal empty pores. In addition, fullerenes and other molecules such as coronene can be entrapped in the empty pores or on the 3NN-Macrocycle molecules. The adsorption constant (K) is estimated, from which it is concluded that the different filling behaviors of the fullerenes are associated with the different sizes of the guest species. This method provides a facile approach to molecularly designed surfaces and the study of fullerene molecular arrays on the single-molecule level.*

Keywords:
- chirality
- fullerenes
- nanoporous materials
- scanning tunneling microscopy
- templates

1. Introduction

Fullerenes have attracted much attention due to their unique physical and chemical properties and potential applications.[1–3] It has been demonstrated that fullerenes form well-ordered adlayers on the surfaces of metals or semiconductors in ultrahigh-vacuum conditions.[4–6] Additionally, fullerene molecules are highly mobile under ambient conditions even when adsorbed on metal surfaces, and have no preferential orientations unless cooled to low temperatures.[7–9] In related topical studies, some porous networks obtained by metal–organic coordination interaction,[10] van der Waals interactions,[11,12] or hydrogen bonds[13] have been successfully used to fabricate ordered fullerene adlayers. There are only a few reported templates that can immobilize fullerenes under ambient conditions so far.[11–13] It is of general interest to develop strategies to achieve highly selective templates which can immobilize fullerene molecules and enable the study of fullerenes at the single-molecule level.

Macrocycles are promising building blocks in fabricating porous networks.[14–17] They can form adlayers when adsorbed onto the surface due to their side groups. The side groups are important to tuning the self-assembly process. The adlayers can entrap guest molecules in the center of the macrocycles[18–21] or the porous networks formed by their side groups.[22,23]

Herein, 1,3,5-tris(10-carboxydecyloxy)benzene (TCDB, Figure 1a) is used as the basic building unit for the host network and 1,2,17,18,33,34-hexaaza-[2$_6$](4,4′)cyclophane-1,17,33-triene[24] (3NN-Macrocycle, Figure 1b) as the guest molecule. We have reported that a kind of quadrangular macrocycle (4NN-Macrocycle) can be immobilized in the TCDB networks and forms different adlayers at different concentrations or with UV irradiation.[25] Here, the two-component system TCDB/3NN-Macrocycle formed a network with nearly sixfold symmetry (C_6) on a highly oriented pyrolitic graphite (HOPG) surface with hexagonal pores. Such a molecular network entrapped guest molecules, such as coronene and fullerene molecules, with notable selectivity. As a result, the size and geometry of the TCDB network cavities could be modulated to appreciably enhance the adsorption efficiency of fullerene molecules.

2. Results and Discussion

TCDB molecules can form an adlayer when deposited on HOPG surfaces. A characteristic structural feature of TCDB is the existence of quasi-rectangular cavities formed by intermolecular hydrogen bonds between carboxyl functionalities of adjacent arms, as shown in Figure 2a. The size of the empty pore is about $2.4 \times 1.3\ nm^2$. We have previously reported

[*] Prof. C. Wang, Q. D. Zeng, Dr. Y.-T. Shen, Dr. K. Deng
National Center for Nanoscience and Technology
11 North First Street, Zhongguancun, Haidian District
Beijing 100190 (P. R. China)
E-mail: wangch@nanoctr.cn; zengqd@nanoctr.cn

Supporting Information is available on the WWW under http://www.small-journal.com or from the author.

DOI: 10.1002/smll.200901601

NANO MICRO small

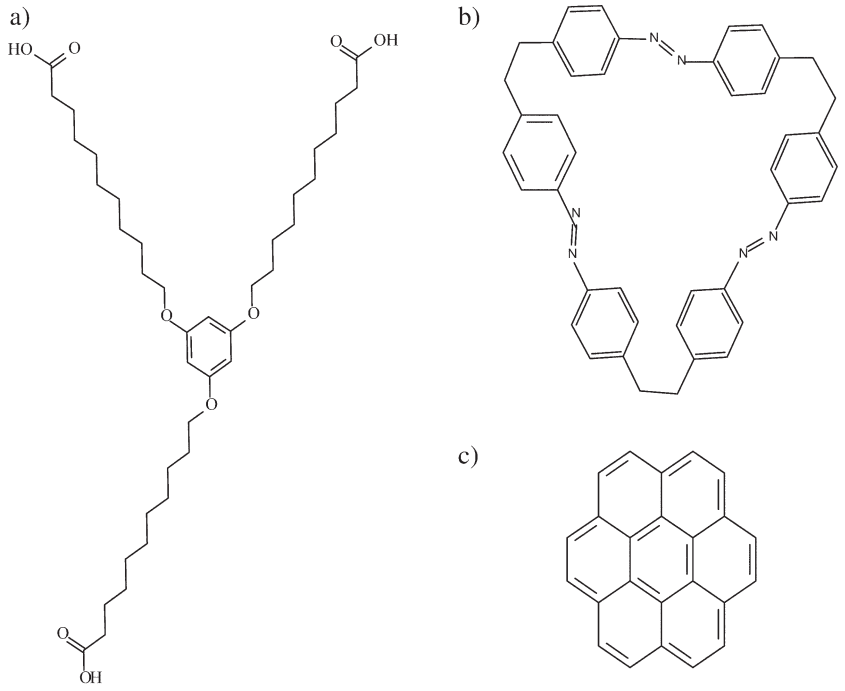

Figure 1. Chemical structures of a) TCDB, b) 3NN-Macrocycle, and c) coronene.

that copper phthalocyanine and coronene molecules can be entrapped in the cavities formed by TCDB to obtain two-component networks.[26,28–29] The size and geometry of the 3NN-Macrocycle are different from those of the unfilled cavities of TCDB. The edge of the triangle is measured to be approximately 2.0 nm.

A large-scale STM image of the TCDB/3NN-Macrocycle adlayer is shown in Figure 2b. The appearance of the adlayer is different from that of the pure TCDB in Figure 2a. The STM images of two chiral molecular patterns are shown in Figure 2c and d, and the details of the entrapped 3NN-Macrocycle molecules are clearly visible. Each hollow bright triangle corresponds to an entrapped triangular macrocycle, indicated as a white triangle in Figure 2b. In Figure 2c and d, three small bright spots can also be observed at the three vertexes of each triangle, which correspond to the benzene cores of three TCDB molecules. Note that the alkyl groups of the three TCDB molecules embrace the 3NN-Macrocycle (Figure 2g and Figure S2, Supporting Information). Two alkyl groups of each TCDB molecule surround a 3NN-Macrocycle molecule, that is to say, six alkyl groups from three TCDB molecules, through three pairs of hydrogen bonds, form a triangular cavity which can entrap a triangular 3NN-Macrocycle. Another alkyl group of the TCDB molecule should be parallel to the adjacent alkyl group and extend to the benzene core of the neighboring TCDB molecule in the empty pore, as shown in Figure S2 (Supporting Information). There are six benzene cores of TCDB in the empty pores.

On the basis of symmetry observations and intermolecular distance, a unit cell is superimposed on the image in Figure 2b and Figure S8 (Supporting Information) with $a = a' = b = b' = 6.3 \pm 0.2$ nm and $\alpha = \alpha' = 60.3 \pm 2.0^{\circ}$. From the molecular model (Figure 2e and f) for the 3NN-Macrocycle molecules entrapped in TCDB networks, it is important to note that each TCDB molecule forms two pairs of hydrogen bonds with two neighboring TCDB molecules and another carboxylic group extends to the benzene core of another adjacent TCDB molecule, because of the C–H···O hydrogen bonds and the van der Waals interaction between the alkyl groups (explained in Figure S9, Supporting Information). Two molecular patterns can be assigned according to the geometrical arrangement of the two-component network from high-resolution STM images, which are designated as R and S, respectively, in Figure 2b–d. A method to distinguish the chiral porous networks is to identify the adjacent 3NN-Macrocycle molecules in a unit, as shown Figure 2e and f. The left-hand 3NN-Macrocycle molecule directs upward and the right-hand one directs downward (marked by the red arrows in Figure 2e), which belongs to type R. Contrarily, another arrangement shown by the red arrows in Figure 2f belongs to type S. From Figure 2e and f, it can be concluded that types R and S cannot be superimposed by rotation and translation operations within the surface plane. This observation indicates that the two-component network of the R and S species possesses chiral characteristics in the adsorption geometry on HOPG.

It is known that generally, the alkyl groups in the empty pore cannot be resolved unambiguously due to conformational fluctuation or co-adsorbed solvent molecules within the pore regions. In order to observe their assembling configuration clearly, we adopted both experimental and theoretical methods to clarify the assembly characteristics (Figure S9, Supporting Information). By introducing coronene molecules into the empty pores, the stability of the alkyl groups was significantly improved. Figure 2g and Figure S3 (Supporting Information) present the inclusion of coronene molecules in the networks. The empty pores of the TCDB/3NN-Macrocycle network are filled by bright circles, which correspond to the coronene molecules. It is observed that there are two parallel alkyl groups between the coronene and the 3NN-Macrocycle molecules. It can be clearly seen that three TCDB molecules embrace one 3NN-Macrocycle, which is consistent with the molecular models in Figure 2e. The six alkyl groups of six TCDB molecules level off the coronenes in the empty pore. The three-component networks also show chirality on the HOPG surface, as shown in Figure S3 (Supporting Information).

The two-component network of the TCDB/3NN-Macrocycle serves as a two-dimensional molecular template that can entrap the fullerenes. When the solution including the fullerenes was dropped onto the two-component network, it was observed that fullerenes were immobilized in the network. Figure 3 and Figures S4–S6 (Supporting Information) exhibit STM images of C_{60}, C_{70}, and C_{80} (D_2) immobilized in the two-component network, respectively. Each bright spot in the empty pores can be associated with an individual molecule of fullerene. From Figures 3a–c, the number of fullerene molecules in the empty pores could be estimated. It is therefore plausible to

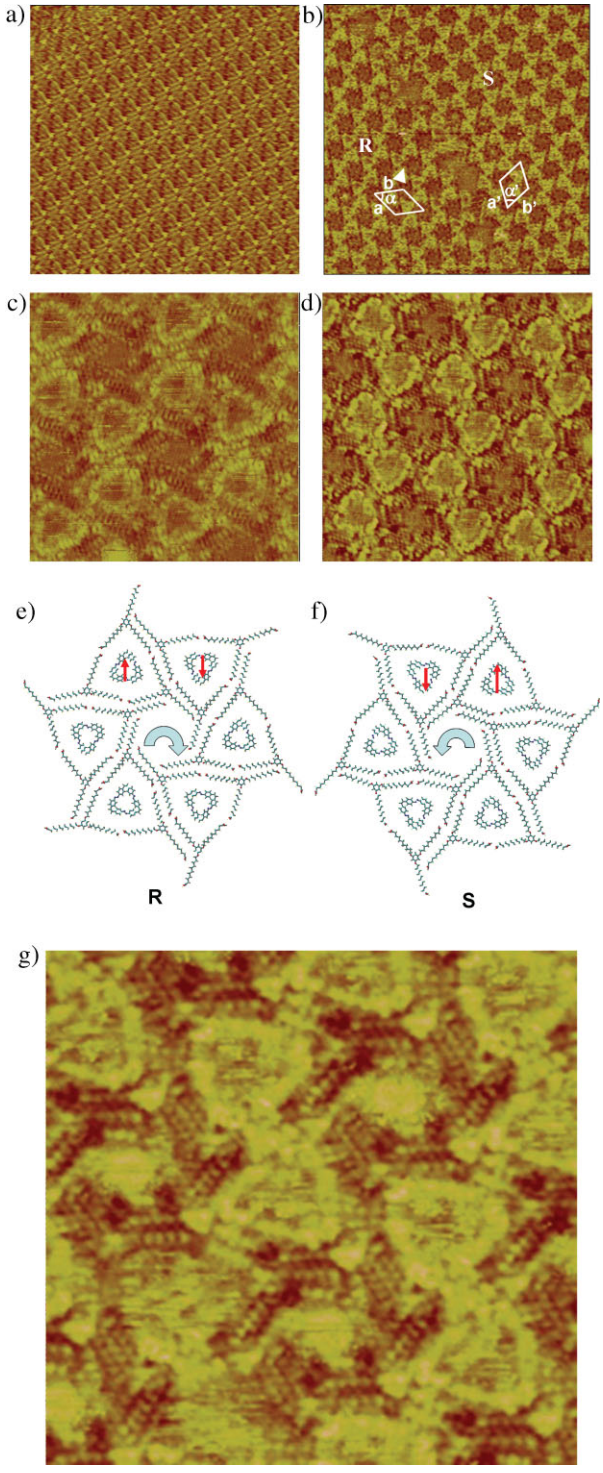

Figure 2. a) STM image ($28 \times 28\,nm^2$, $I = 299$ pA, $V = 649$ mV) of the TCDB adlayers on a HOPG surface. b) Large-scale STM image ($55 \times 55\,nm^2$, $I = 293$ pA, $V = 700$ mV) of the TCDB networks modulated by 3NN-Macrocycle on a HOPG surface. c) High-resolution STM image of the type R TCDB/3NN-Macrocycle adlayer ($14 \times 14\,nm^2$, $I = 335$ pA, $V = 553$ mV). d) High-resolution STM image of the type S TCDB/3NN-Macrocycle adlayer ($18 \times 18\,nm^2$, $I = 467$ pA, $V = -700$ mV). e) R-type molecular model for the two-component network. f) S-type molecular model for the two-component network. g) High-resolution image of the R-type TCDB/3NN-Macrocycle/coronene networks. A bright circular molecule is observed in the pore, which corresponds to the coronene ($13 \times 13\,nm^2$, $I = 1016$ pA, $V = 591$ mV).

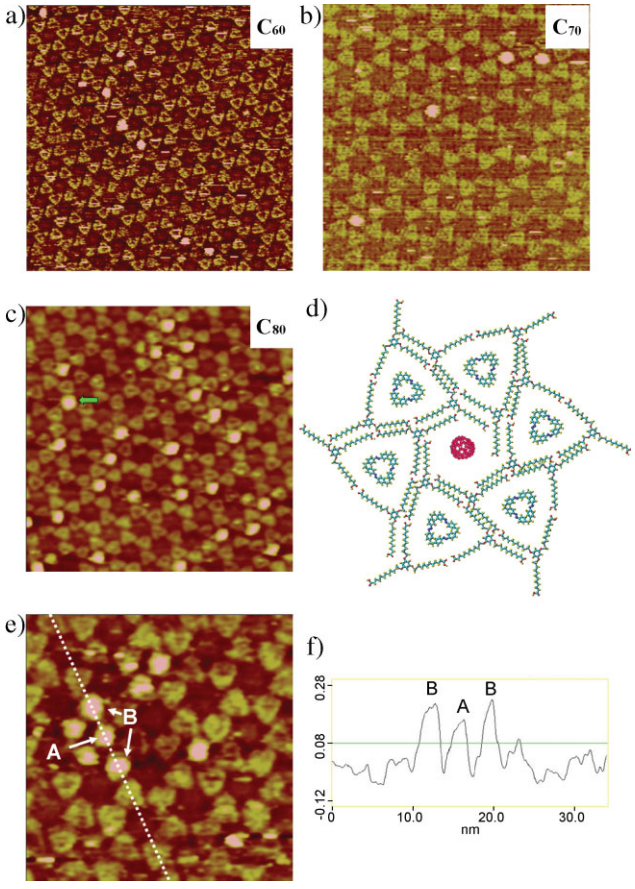

Figure 3. a–c) Large-scale STM images of C_{60}, C_{70}, and C_{80} entrapped in the empty pores on the HOPG surface, respectively. The molecules are entrapped in the two-component network: a) $65 \times 65\,nm^2$, $I = 269$ pA, $V = 1191$ mV; b) $47 \times 47\,nm^2$, $I = 214$ pA, $V = 1188$ mV; c) $52 \times 52\,nm^2$, $I = 214$ pA, $V = 1172$ mV. Green arrow in (c): fullerene molecules on top of 3NN-Macrocycle molecules. d) Molecular model of the C_{80} molecules entrapped in empty pores of the two-component network. e) STM image of C_{80} molecules entrapped in empty pores and on the 3NN-Macrocycle ($31 \times 31\,nm^2$, $I = 284$ pA, $V = 1206$ mV). f) Cross-sectional profile of the dotted line indicated in (e). The three peaks correspond to the three C_{80} molecules marked in (e).

suggest that the different filling behaviors of the fullerenes are associated with the different sizes of the guest species.

To demonstrate the different filling behavior we performed experiments in which the concentration of C_{60}, C_{70}, and C_{80} was controlled at about 8.3×10^{-8} mol mL^{-1}. Figure 4 presents the adsorption densities of the fullerenes (determined by the ratio of the number of entrapped fullerenes to the number of all pores including the filled and unfilled pores in the STM images). It shows that the adsorption density of C_{80} is appreciably higher than that of C_{60} and C_{70}. We estimated the typical area of HOPG in our study to be $3 \times 3\,mm^2$ and the area of a unit as about $34.3\,nm^2$. So the number of empty pores is about 2.6×10^{11}. A droplet of approximately 0.8 μL solution (about 8.3×10^{-8} mol mL^{-1}) deposited on the surface contains about 4.0×10^{13} fullerene molecules. We conclude that the crude estimation of the ratio between the molecular number on the surface and the molecular number in solution is about 1.6×10^{-4} (C_{60}, C_{70}) and 1.6×10^{-3} (C_{80}). By carefully observing the images we found that a few fullerene molecules are on top of the

NANO MICRO small

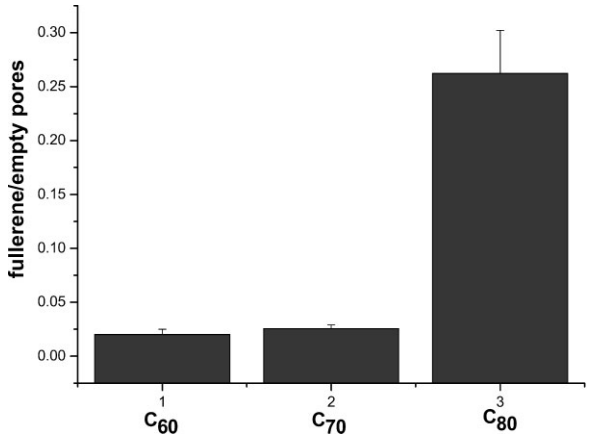

Figure 4. Statistical graph of the fullerene/empty pores showing the different filling ratios of the entrapped fullerene molecules versus all the empty pores (including filled and unfilled pores).

3NN-Macrocycle molecules, as indicated by the green arrow in Figure 3c. Figure 3e is an STM image that contains three adjacent C_{80} molecules. Figure 3f is a cross-sectional profile of the indicated line in Figure 3e. The profile shows that the height of the fullerene on the macrocycles is higher than that in the empty pores. It can be concluded that two molecules (marked B) are sitting on top of a 3NN-Macrocycle.

Careful examination of Figure 3a enables the observation that empty pores could contain some unidentified species in the experiments. Such an effect may be due to the co-adsorption of solvent molecules, as illustrated in a number of previous studies.[30–32] We consider that the size of fullerenes is a key to the immobilization process. This study demonstrates that different fullerenes can be size-selectively immobilized in the co-assembled molecular network. We conclude that the adsorption behavior of fullerenes in the empty pores is dependent on the total interaction energy, which is consistent with the experimental results.

The selectivity of the immobilization process was supported by the difference in total energy of the adsorbed molecules. According to theoretical calculations, the average interaction energy for the C_{80}–empty pore–graphite system ($E_{\text{empty pore}}$) is -112.11 kJ mol^{-1}, which is less than that of C_{70} (-96.73 kJ mol^{-1}) and C_{60} (-89.33 kJ mol^{-1}) entrapped in the empty pores, as shown in the first row of Table 1. This result indicates a strong interaction in the C_{80}–pore–graphite system. Thus, C_{80} molecules have higher stability in empty pores than the other two fullerenes. Additionally, the absolute value of the energy of fullerenes on top of the 3NN-Macrocycle ($E_{\text{3NN-Macrocycle}}$) is less than that in the empty pores ($E_{\text{empty pore}}$; Table 1), which indicates that the fullerenes are predominantly adsorbed in the empty pores of the TCDB/3NN-Macrocycle network. So the number of fullerene molecules entrapped in the empty pores is more than that on the macrocycles.

In fact, the adsorbed amount of fullerene Q_e (e = entrapped) would be increased toward a line as the concentration C_e of the fullerene solution was increased according to the Langmuir equation $Q_e = KC_e$ for extremely dilute solution concentrations, where K is the adsorption constant. The plot of C_e versus Q_e is shown in Figure 5, where the slope is the adsorption constant K. The resulting K values are listed in Table 1. Note that the value of K_{80} is much higher than that of K_{70} and K_{60}. The $K_{\text{fullerenes}}$ are all more than 1, which indicates that the process of adsorption is a spontaneous process.

Table 1. Total interaction energies for fullerene depositing on the 3NN-Macrocycle (third row) and in the empty pore (first row). The difference of the interaction energies for the fullerene based on C_{60} in pores is shown in the second row. The total energy ($E_{\text{empty pore}}$) includes the interaction energy of fullerene–empty pore and fullerene–graphite (kJ mol^{-1}). K is the adsorption constant, which is obtained from Figure 5 (dm^3 mol^{-1}).

	C_{80}	C_{70}	C_{60}
$E_{\text{empty pore}}$	−112.11	−96.73	−89.33
$E_{80\text{ or }70}-E_{60\text{ (empty pore)}}$	−22.78	−7.4	–
$E_{\text{on top of 3NN-Macrocycle}}$	−86.44	−56.67	54.49
K	1 059 100	612 800	550 400

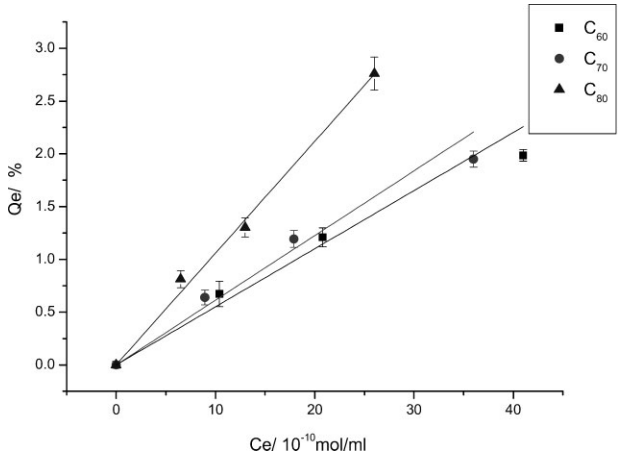

Figure 5. Adsorption isotherms of fullerenes in heptanoic acid.

3. Conclusions

Compared with the packing pattern of pure TCDB, significantly different characteristics were observed using STM under ambient conditions for the co-assembly structure of TCDB/3NN-Macrocycle. The pristine TCDB networks and the macrocycle molecules are achiral molecules. The adlayer of TCDB affected by 3NN-Macrocycle becomes a two-component chiral network, which can immobilize coronene molecules. Additionally, the presented results illustrate that the co-assembled supramolecular network effectively immobilized fullerene molecules with appreciable size selectivity. The observed different filling behaviors for the fullerenes are associated with the different sizes of the guest species, which are reflected by the adsorption constant K and the theoretical calculations as shown in Table 1. The method provides a facile approach to surface modification and the fabrication of novel hierarchical molecular structures.

4. Experimental Section

Sample preparation: TCDB and 3NN-Macrocycle were synthesized by the method reported previously.[24,26] The C_{80} (D_2) was

synthesized and separated by following previously reported methods.[27] C_{60} was purchased from Alfa Co. and used as received. Coronene (97%) and C_{70} (96%) were purchased from Aldrich Co. and used as received. The solvent used in the STM experiments was heptanoic acid (HPLC grade, Acros Co.). The concentrations of the solutions of TCDB and 3NN-Macrocycle were about 1.0×10^{-7} mol mL^{-1}. The molar ratio of TCDB to 3NN-Macrocycle was approximately 3:1. The concentration of the coronene solution was about 1.0×10^{-7} mol mL^{-1}. The concentration of the C_{60}, C_{70}, and C_{80} was about 8.3×10^{-8} mol mL^{-1}, and was used to obtain Figure 4. Figure 5 was obtained from solutions with the following concentrations: C_{60}: about 1.04×10^{-9}, 2.08×10^{-9}, and 4.1×10^{-9} mol mL^{-1}; C_{70}: about 8.9×10^{-10}, 1.8×10^{-9}, and 3.6×10^{-9} mol mL^{-1}; and C_{80}: about 6.5×10^{-10}, 1.3×10^{-9}, and 2.6×10^{-9} mol mL^{-1}.

STM: Heptanoic acid is electrically nonconductive and its vapor pressure at room temperature is low enough to allow stable tunneling experiments over extended times after deposition on a graphite surface. The samples were prepared in two steps. First, a droplet of solution containing TCDB and the 3NN-Macrocycle compounds (3:1) was deposited on freshly cleaved HOPG surfaces. The HOPG was placed on a temperature controller (Lake Shore 321). Then the sample was annealed at 60 °C and kept for about 20 min until the two-component network was fabricated on the HOPG surface. Second, a droplet of the solution of coronene in heptanoic acid was added to the prepared two-component network. TCDB/3NN-Macrocycle/coronene three-component networks were fabricated on the HOPG surface. The fabrication process of the TCDB/3NN-Macrocycle/fullerenes (C_{60}, C_{70}, C_{80}) was similar. STM measurements were performed at room temperature with a Nanoscope IIIA system (Veeco Metrology, USA). All STM images were recorded in the constant-current mode. The specific tunneling conditions are given in the figure captions. All the experiments were performed at the heptanoic acid/HOPG interface.

Acknowledgements

Financial support from the Knowledge Innovation Program of the Chinese Academy of Sciences (Grant No. KJCX2-YW-MO4), National Natural Science Foundation of China (Grant no. 50602007) and the National Key Project for Basic Research (grant nos. 2007CB936503 and 2006CB932104) is gratefully acknowledged. We also thank Dr. Ai-Fang Yu, Ms. Yan-Li Wang, Prof. Bao-Hang Han, and Dr. Ye-Ping Jiang for their help with adsorption experiments.

[1] P. M. Allemand, K. C. Khemani, A. Koch, F. Wudl, K. Holczer, S. Donovan, G. Gruner, J. D. Thompson, *Science* **1991**, *253*, 301–303.
[2] N. Katsonis, A. Marchenko, D. Fichou, *J. Photochem. Photobiol. A* **2003**, *158*, 101–104.
[3] N. S. Sariciftci, L. Smilowitz, A. J. Heeger, F. Wudl, *Science* **1992**, *258*, 1474–1476.
[4] J. A. Theobald, N. S. Oxtoby, M. A. Phillips, N. R. Champness, P. H. Beton, *Nature* **2003**, *424*, 1029–1031.
[5] L. F. Yuan, J. L. Yang, H. Q. Wang, C. G. Zeng, Q. X. Li, B. Wang, J. G. Hou, Q. S. Zhu, D. M. Chen, *J. Am. Chem. Soc.* **2003**, *125*, 169–172.
[6] J. G. Hou, J. L. Yang, H. Q. Wang, Q. X. Li, C. G. Zeng, L. F. Yuan, B. Wang, D. M. Chen, Q. S. Zhu, *Nature* **2001**, *409*, 304–305.
[7] X. H. Lu, M. Grobis, K. H. Khoo, S. G. Louie, M. F. Crommie, *Phys. Rev. Lett.* **2003**, *90*, 096802.
[8] M. Abel, A. Dmitriev, R. Fasel, N. Lin, J. V. Barth, K. Kern, *Phys. Rev. B* **2003**, *67*, 245407.
[9] T. Hashizume, K. Motai, X. D. Wang, H. Shinohara, Y. Saito, Y. Maruyama, K. Ohno, Y. Kawazoe, Y. Nishina, H. W. Pickering, Y. Kuk, T. Sakurai, *Phys. Rev. Lett.* **1993**, *71*, 2959–2962.
[10] S. Stepanow, M. Lingenfelder, A. Dmitriev, H. Spillmann, E. Delvigne, N. Lin, X. B. Deng, C. Z. Cai, J. V. Barth, K. Kern, *Nat. Mater.* **2004**, *3*, 229–233.
[11] S. Yoshimoto, E. Tsutsumi, R. Narita, Y. Murata, M. Murata, K. Fujiwara, K. Komatsu, O. Ito, K. Itaya, *J. Am. Chem. Soc.* **2007**, *129*, 4366–4376.
[12] H. Glowatzki, B. Bröker, R. P. Blum, O. T. Hofmann, A. Vollmer, R. Rieger, K. Müllen, E. Zojer, J. P. Rabe, N. Koch, *Nano Lett.* **2008**, *8*, 3825–3829.
[13] M. Li, K. Deng, S. B. Lei, Y. L. Yang, T. S. Wang, Y. T. Shen, C. R. Wang, Q. D. Zeng, C. Wang, *Angew. Chem.* **2008**, *120*, 6819–6823; *Angew. Chem. Int. Ed.* **2008**, *47*, 6717–6721.
[14] J. Vicario, T. Kudernac, J. Visser, M. M. Pollard, B. L. Feringa, *J. Am. Chem. Soc.* **2006**, *128*, 15537–15541.
[15] A. Ziegler, W. Mamdouh, A. V. Heyen, M. Surin, H. Uji-i, M. M. S. Abdel-Mottaleb, F. C. De Schryver, S. De Feyter, R. Lazzaroni, S. Höger, *Chem. Mater.* **2005**, *17*, 5670–5683.
[16] V. Kalsani, H. Ammon, F. Jäckel, J. P. Rabe, M. Schmittel, *Chem. Eur. J.* **2004**, *10*, 5481–5492.
[17] S. Höger, K. Bonrad, A. Mourran, U. Beginn, M. Möller, *J. Am. Chem. Soc.* **2001**, *123*, 5651–5659.
[18] B. Schmaltz, A. Rouhanipour, H. J. Räder, W. Pisula, K. Müllen, *Angew. Chem.* **2009**, *121*, 734–738; *Angew. Chem. Int. Ed.* **2009**, *48*, 720–724.
[19] K. Tahara, S. Lei, W. Mamdouh, Y. Yamaguchi, T. Ichikawa, H. Uji-i, M. Sonoda, K. Hirose, F. C. De Schryver, S. De Feyter, Y. Tobe, *J. Am. Chem. Soc.* **2008**, *130*, 6666–6667.
[20] E. Mena-Osteritz, P. Bäuerle, *Adv. Mater.* **2006**, *18*, 447–451.
[21] G. B. Pan, X. H. Cheng, S. Höger, W. Freyland, *J. Am. Chem. Soc.* **2006**, *128*, 4218–4219.
[22] S. Furukawa, K. Tahara, F. C. De Schryver, M. Van der Auweraer, Y. Tobe, S. De Feyter, *Angew. Chem.* **2007**, *119*, 2889–2892; *Angew. Chem. Int. Ed.* **2007**, *46*, 2831–2834.
[23] S. Lei, K. Tahara, X. Feng, S. Furukawa, F. C. De Schryver, K. Müllen, Y. Tobe, S. De Feyter, *J. Am. Chem. Soc.* **2008**, *130*, 7119–7129.
[24] R. Tamaoki, K. Ogata, K. Koseki, T. Yamaoka, *Tetrahedron* **1990**, *46*, 5931–5942.
[25] Y. T. Shen, L. Guan, X. Y. Zhu, Q. D. Zeng, C. Wang, *J. Am. Chem. Soc.* **2009**, *131*, 6174–6180.
[26] J. Lu, S. B. Lei, Q. D. Zeng, S. Z. Kang, C. Wang, L. J. Wan, C. L. Bai, *J. Phys. Chem. B* **2004**, *108*, 5161–5165.
[27] F. H. Hennrich, R. H. Michel, A. Fischer, S. Richard-Schneider, S. Gilb, M. M. Kappes, D. Fuchs, M. Burk, K. Kobayashi, S. Nagase, *Angew. Chem.* **1996**, *108*, 1839–1841; *Angew. Chem. Int. Ed.* **1996**, *35*, 1732–1734.
[28] X. H. Kong, K. Deng, Y. L. Yang, Q. D. Zeng, C. Wang, *J. Phys. Chem. C* **2007**, *111*, 9235–9239.
[29] X. H. Kong, K. Deng, Y. L. Yang, Q. D. Zeng, C. Wang, *J. Phys. Chem. C* **2007**, *111*, 17382–17387.
[30] K. Tahara, S. Furukawa, H. Uji-i, T. Uchino, T. Ichikawa, J. Zhang, W. Mamdouh, M. Sonoda, F. C. De Schryver, S. De Feyter, Y. Tobe, *J. Am. Chem. Soc.* **2006**, *128*, 16613–16625.
[31] L. Piot, C. Marie, X. Feng, K. Müllen, D. Fichou, *Adv. Mater.* **2008**, *20*, 3854–3858.
[32] W. Mamdouh, H. Uji-i, J. S. Ladislaw, A. E. Dulcey, V. Percec, F. C. De Schryver, S. De Feyter, *J. Am. Chem. Soc.* **2006**, *128*, 317–325.

Received: August 26, 2009
Published online: November 10, 2009

